

Multiple Potentials of Mean Force from Biased Experiments Along a Single Coordinate

David D.L. Minh

February 8, 2020

Department of Chemistry and Biochemistry and Center for Theoretical Biological Physics, University of California at San Diego, San Diego, California 92093

Abstract

External biasing forces are often applied to enhance sampling in regions of phase space which would otherwise be rarely observed. While the typical goal of these experiments is to calculate the potential of mean force (PMF) along the biasing coordinate, here I present a method to construct PMFs in multiple dimensions and along arbitrary alternative degrees of freedom. A formalism for multidimensional PMF reconstruction from nonequilibrium single-molecule pulling experiments is introduced and tested on a series of two dimensional potential surfaces with varying levels of correlation. Reconstruction accuracy and convergence from several methods - this new formalism, equilibrium umbrella sampling, and free diffusion - are compared, and nonequilibrium pulling is found to be the most efficient.

1 Introduction

External biasing forces are often applied to enhance sampling in regions of phase space which would otherwise be rarely observed.¹ These perturbing forces are applied in both time-dependent, as in single-molecule pulling²⁻⁵ and steered molecular dynamics^{6,7} experiments, or time-independent forms, as in umbrella sampling simulations.⁸ Usually, the direction of bias is chosen to follow the reaction coordinate for an interesting process, such as a large conformational change in a biological macromolecule. With judicious reweighing of biased ensemble properties, previous workers have reconstructed the potential of mean force (PMF) along this bias coordinate.⁹⁻¹⁴

The ability to reconstruct PMFs in multiple dimensions and along multiple alternative degrees of freedom would significantly expand the data analysis tool kit for biased experiments. Although the appropriate choice of reaction coordinate is fundamental to kinetic calculations, transition state theory, and the accurate separation of distinct microstates, its selection is limited by prior knowledge of the system. It would be useful to compute PMFs along alternate potential reaction coordinates, in one or several dimensions, after biased data is collected along an initial, somewhat arbitrary choice. In addition, by using multidimensional PMFs, the mutual entropy¹⁵ can be used to quantify and compare correlations between modes. Here, I develop methods to perform these calculations. They are applicable to both computer simulations, in which system properties are completely known, or laboratory experiments in which several properties are simultaneously measured.

2 The Potential of Mean Force

The PMF, $F_0(x)$, along a single coordinate, x , is defined as

$$e^{-\beta[F_0(x)+\delta F]} = \frac{\int \delta[x - x(\mathbf{r})] e^{-\beta\{H_0(\mathbf{r})\}} d\mathbf{r}}{\int e^{-\beta\{H_0(\mathbf{r}')\}} d\mathbf{r}'} \quad (1)$$

where δF is an arbitrary constant, β is $1/k_b T$, and $H_0(\mathbf{r})$ is the unperturbed system energy as a function of the phase space position \mathbf{r} .

In two dimensions, $F_0(x)$ becomes $F_0(x, y)$ and $\delta[x - x(\mathbf{r})]$ is replaced by $\delta[x - x(\mathbf{r})]\delta[y - y(\mathbf{r})]$. Generalizing to multiple dimensions, $F_0(x)$ becomes $F_0(x, y_1, y_2, \dots, y_n)$ and the delta function is replaced by $\delta[x - x(\mathbf{r})]\prod_{i=1}^n \delta[y_i - y_i(\mathbf{r})]$, where n is the number of dimensions. If the PMF encompasses all system dimensions, it can simply be referred to as the potential.

3 Multidimensional PMFs from Nonequilibrium Experiments

Multidimensional PMFs can be reconstructed from time-dependent biasing experiments by applying the nonequilibrium work relation^{16,17} in a manner analogous to Hummer and Szabo.^{11,12} In a single-molecule pulling experiment with the Hamiltonian $H(\mathbf{r}, t) = H_0(\mathbf{r}) + V[\mathbf{r}, t]$, where $V[\mathbf{r}, t]$ is the time-dependent external bias, the biased probability density function is

$$\frac{e^{-\beta\{H_0(\mathbf{r})+V[\mathbf{r},t]\}}}{\int e^{-\beta\{H_0(\mathbf{r}')+V[\mathbf{r}',0]\}} d\mathbf{r}'} = \langle \delta(\mathbf{r} - \mathbf{r}(t))e^{-\beta W_t} \rangle \quad (2)$$

where W_t is the accumulated work, $\int_0^t \frac{\partial H(\mathbf{r}, t')}{\partial t'} dt'$.^{11,12}

To calculate the PMF along the pulling coordinate, Hummer and Szabo consider the special case that the perturbation depends only on the biasing coordinate and time, $V(\mathbf{r}, t) = V[x(\mathbf{r}), t]$. They then multiply equation 2 by $e^{\beta V(x,t)}\delta[x - x(\mathbf{r})]$, integrate over all phase space, and use the definition in equation 1 to obtain

$$e^{-\beta F_0(x)} = \langle \delta(x - x(\mathbf{r}))e^{-\beta(W_t - V[x,t])} \rangle \quad (3)$$

If we instead multiply equation 2 by a two-dimensional delta function, we then obtain the two-dimensional PMF. Similarly, multiplying by a multidimensional delta function will lead to a multidimensional PMF. In

the two-dimensional case, the PMF is

$$e^{-\beta F_0(x,y)} = \langle \delta(x - x(\mathbf{r}))\delta(y - y(\mathbf{r}))e^{-\beta(W_t - V[x,t])} \rangle \quad (4)$$

In any single time slice, the position will be more highly sampled near the minima of the bias potential. To improve accuracy over the entire range of x , data from different time slices can be combined by adapting the weighted histogram analysis method (WHAM).⁹ After unbiasing with respect to the accumulated work as well as the time-dependent potential,^{11,12} the resultant PMF is

$$F_o(x) = -\beta^{-1} \ln \frac{\sum_t \frac{\langle \delta(x - x(\mathbf{r}))\delta(y - y(\mathbf{r}))e^{-\beta W_t} \rangle}{\langle e^{-\beta W_t} \rangle}}{\sum_t \frac{e^{-\beta V(x,t)}}{\langle e^{-\beta W_t} \rangle}} \quad (5)$$

4 Correlation

The usefulness of reconstructing y from experiments biased along x is expected to be related to their degree of correlation. One standard measure for the correlation of two coordinates with known probability density, $f(x, y)$, is the mutual entropy,¹⁵

$$S_{mutual} = \int \int f(x, y) \log \frac{f(x, y)}{f(x)f(y)} dx dy \quad (6)$$

where $f(x)$ and $f(y)$ are the marginal probabilities along x and y . If x and y are completely independent, $f(x, y) = f(x)f(y)$ and the mutual entropy is zero. In this case, a naive estimate of the PMF along y , $F(y) = -k_b T \ln(f(y))$, should be as good as a reconstruction from equation 5. If x and y are highly correlated, then the mutual entropy should be high. The naive estimate will fail, making the value of equation 5 more evident.

Equation 5 was tested on series of two-dimensional potential surfaces consisting of a linear combination

of

$$U_a(x, y) = 5x^2(x - 45)^2 + 1.7 \times 10^{-4}y^2(y - 30)^2 \quad (7)$$

and

$$U_b(x, y) = 15 \ln[(2x - 3y)^2 + 100] + 1.25 \times 10^{-7}(2x + 3y)^2(2x + 3y - 180)^2 \quad (8)$$

according to

$$U(x, y, \alpha) = \alpha U_a + (1 - \alpha) U_b \quad (9)$$

where U is in units of $pN \cdot nm$ and positions x and y are in units of nm . U_a and U_b both have minima at $(0,0)$ and $(45,30)$, and U_a has additional minima at $(0,30)$ and $(45,0)$. In U_a (Fig. 5c), x and y are completely independent, while in U_b (Fig. 2c), they are highly correlated. This is quantified by the mutual entropy (Fig. 1), which was calculated by assuming a Boltzmann distribution for x and y , $f(x, y) = e^{-\beta U(x, y)}$, and numerically integrating equation 6 between $-20 < x < 65$ and $-20 < y < 50$ via adaptive Simpson quadrature.

As expected, mutual entropy decreases as the potential becomes more like U_a . The joint entropy, $S_{xy} = \int f(x, y) dx dy$, and the marginal entropies, $S_x = \int f(x) dx$ and $S_y = \int f(y) dy$, are mostly stable as a function of α . These magnitude of these factors cannot be directly compared to the mutual entropy because they are offset by an arbitrary constant, whereas mutual entropy is invariant to scale.

5 Simulations on a Two-Dimensional Energy Surface

Brownian dynamics simulations¹⁸ were run on the series of potential surfaces. The progress of a dynamical variable is given by $x(t) = \frac{F(x(t-1))D\Delta t}{k_b T} + (2D\Delta t)^{1/2}R$, where $F(x) = \frac{-\partial U(x, y)}{\partial x}$ is the force, T is the

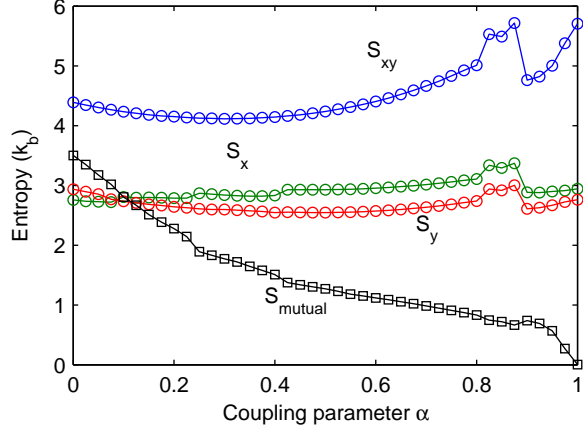


Figure 1: Entropy as a function of the coupling parameter α . The mutual entropy, S_{mutual} , is designated by connected squares. The joint entropy, S_{xy} , and the marginal entropies, S_x and S_y , are labeled and marked by connected circles.

temperature (300 K), D is the diffusion constant (1200 nm^2/s), Δt is the time step (1 ms), and R is a normally distributed random variable.

After 1000 steps of equilibration, biased simulations were run for 100 iterations of 10000 time steps. In addition, 10 unbiased diffusion simulations were run for 100000 time steps. Umbrella sampling was performed with a harmonic bias, $V(x(\mathbf{r})) = 1/2k_s(b-x(\mathbf{r}))^2$, setting the spring constant, k_s , at 0.1 pN/nm and the bias center, b , at one of 100 evenly spaced positions between -5 and 50 nm. Pulling simulations were performed with the time-dependent perturbation, $V[x(\mathbf{r}), t] = 1/2k_s(b(t) - x(\mathbf{r}))^2$, with k_s set to 0.4 pN/nm . A periodic biasing program,¹⁹ $b(t) = 22.5 - 27.5 \cos(2\pi t/10000)$, which has one period per trajectory, was used. Accumulated work was numerically integrated by $W_t = \sum_{j=1}^t -k_s[(x_j + x_{j-1})/2 - (b_j + b_{j-1})/2](b_j - b_{j-1})$, where b_j is the position of the bias center at time step j .

Theoretical surfaces, $U(x)$ and $U(y)$, were calculated by assuming a Boltzmann distribution, $f(x, y) = e^{-\beta U(x, y)}$, and numerically integrating $f(x, y)$ over the other coordinate (with limits of $-20 < x < 65$ and $-20 < y < 50$) using adaptive Simpson quadrature to obtain a marginal probability density. PMFs are then obtained by taking natural logarithms and multiplying by $-k_b T$. In time-dependent biasing experiments, reconstructed surfaces for x were calculated using equation 3, two-dimensional surfaces from equation 4, and surfaces along y by integrating over x ; from the estimate of $f(x, y)$, the sum is taken over x to yield an unnormalized $f(y)$, from which $U(y) = -k_b T \ln f(y)$ is calculated. PMFs from umbrella sampling were

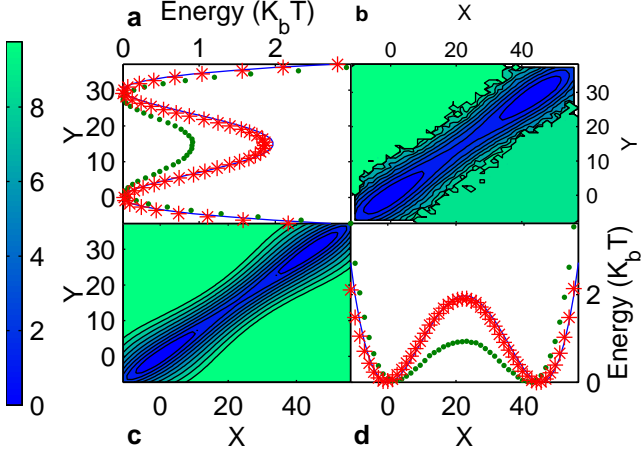


Figure 2: PMF reconstruction on the surface with $\alpha = 0$ from umbrella sampling. **a.** PMFs along the y coordinate. The blue line is the theoretical surface, the red asterisks are the biased reconstruction, and green dots are the naive reconstruction. **b.** Contour plot of PMF reconstruction. **c.** Contour plot of the theoretical PMF. The scale for both b and c and indicated by the side color bar. **d.** PMFs along the x coordinate. Annotation is the same as in **a**.

calculated as described by Roux.¹⁰ Minima of all PMFs were set to zero. Errors were calculated by the root mean square deviation from the theoretical surface at 50 points between $-10.9091 < x < 55.9091$ and $7.2727 < y < 37.2727$, ranges which include the zeroes of U_a and U_b .

6 Results and Discussion

When x and y are completely independent, the naive estimate for $F(y)$ is as good as the estimate from equation 5 (Fig. 5a). If x and y are highly correlated, however, the naive estimate fails and a WHAM-informed reconstruction method is necessary (Fig. 2). This trend is clear from observing the root mean square error as a function of mutual entropy (Fig. 6).

There is no simple dependence, however, between error and mutual entropy, as other factors of the free energy surface come into play. For example, on certain free energy surfaces, phase space sampling along the y dimension may be limited by trapping in local minima. Indeed, sampling is generally limited in high-energy regions of phase space (see Figs. 2, 3, 4, and 5). For these regions, the most accurate two-dimensional PMF reconstruction would require biasing along both x and y . Due to the highly diffusive nature of the dynamics and the large timestep necessary for fast sampling, however, sampling is erroneously

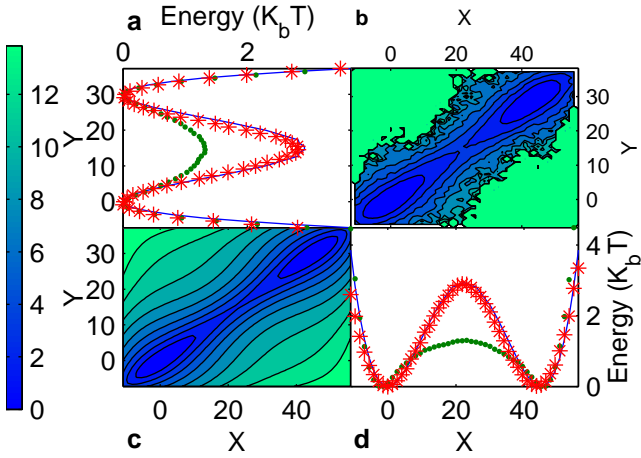


Figure 3: PMF reconstruction on the surface with $\alpha = 0.3$ from time-dependent biasing experiments. Annotation is the same as in Figure 2.

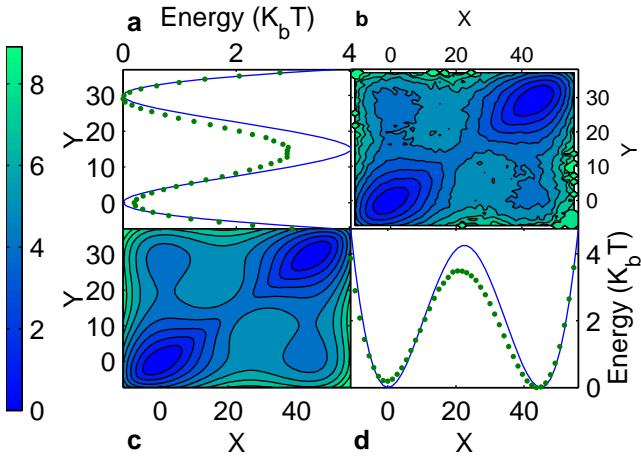


Figure 4: PMF reconstruction on the surface with $\alpha = 0.75$ from diffusion experiments. Annotation is the same as in Figure 2, except there are no WHAM reconstructions.

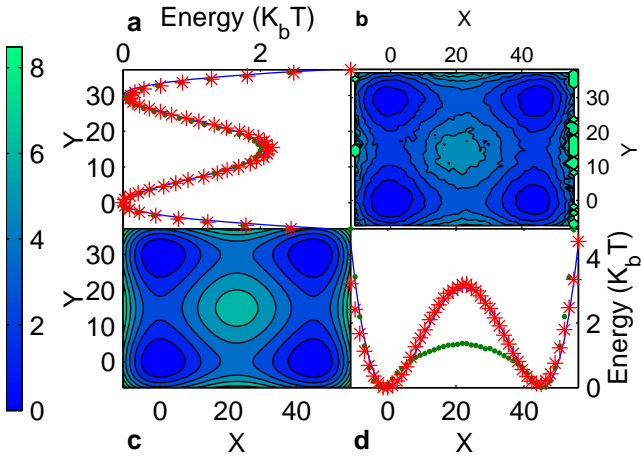


Figure 5: PMF reconstruction on the surface with $\alpha = 1.0$ from time-dependent biasing experiments. Annotation is the same as in Figure 2.

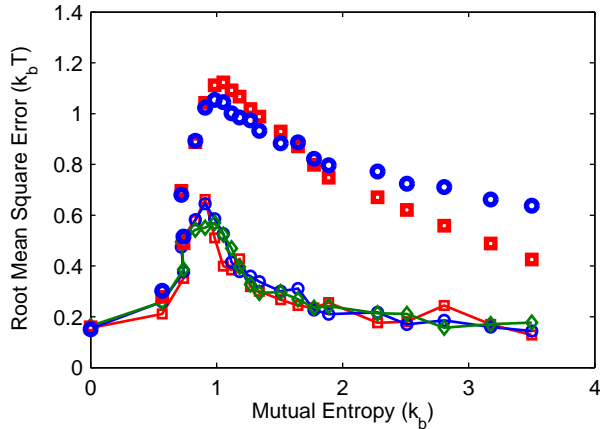


Figure 6: Root mean square error as a function of mutual entropy. Reconstruction errors for pulling experiments are indicated by squares and for umbrella sampling by circles. Errors in WHAM-reconstructed surfaces are connected by solid lines, while the naive estimate errors are not connected.

improved near the boundaries of small low-energy wells, leading to systematic free energy underestimates (Fig. 4) in all simulations.

On the toy two-dimensional surfaces studied, the new method using equation 5 actually converges more quickly than equilibrium umbrella sampling and reconstruction from unbiased experiments 7. While time-dependent biasing experiments will sample the whole span of the bias coordinate *de facto*, umbrella sampling will inherently require a certain number of simulations at different bias centers to attain this sampling. Similarly, unbiased simulations will need to be run for longer in order to reach more distal regions of phase space. Generally, it is preferable to run a greater number of nonequilibrium experiments than a single long equilibrium experiment because the outcome of each individual trajectory can be highly dependent on initial conditions. These sampling problems illustrated in the two-dimensional surface are likely to be enhanced in systems with higher complexity. The main caveat with this method, as with all methods based on the nonequilibrium work relation, is that with greater free energy differences, the likelihood of observing a trajectories with negative dissipative work (work is less than the free energy difference) is increasingly unlikely.

For these reasons, biased experiments are poised to find broader utility in studies of nanoscale systems, particularly when free energy differences between states are not prohibitively large. I hope this analysis tool will find wide application in these computational and laboratory experiments.

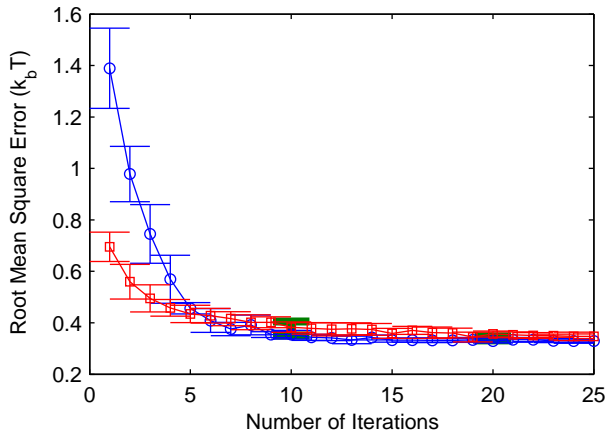


Figure 7: Root mean square error (RMSE) as a function of number of simulations. Error bars indicate the mean and standard deviations of RMSE from five reconstructions using various sample sizes over all tested free energy surfaces. Reconstruction errors for pulling experiments are indicated by squares and for umbrella sampling by circles. Unbiased simulations, which were run for 10 times as long, are therefore spaced 10 times farther apart on the x axis.

7 acknowledgments

I would like to thank R. Amaro, C.E. Chang, J. Gullingsrud, K. Lindenberg, and J.A. McCammon for helpful discussions. I am funded by the NIH Molecular Biophysics Training Grant at UCSD. McCammon group resources are supported by the NSF (MCB-0506593), NIH (GM31749), HHMI, CTBP, NBCR, W.M. Keck Foundation, and Accelrys, Inc.

References

- [1] Adcock, S.; McCammon, J. *Chem. Rev.*, **2006**, *106*, 1589–1615.
- [2] Perkins, T.; Smith, D.; Chu, S. *Science*, **1994**, *264*(5160), 819–822.
- [3] Florin, E.; Moy, V.; Gaub, H. *Science*, **1994**, *264*(5157), 415–417.
- [4] Strick, T.; Allemand, J.; Bensimon, D.; Bensimon, A.; Croquette, V. *Science*, **1996**, *271*, 1835–1837.
- [5] Smith, S.; Cui, Y.; Bustamante, C. *Science*, **1996**, *271*, 795–799.
- [6] Isralewitz, B.; Gao, M.; Schulten, K. *Curr. Opin. Struct. Biol.*, **2001**, *11*(2), 224–230.

- [7] Isralewitz, B.; Baudry, J.; Gullingsrud, J.; Kosztin, D.; Schulten, K. *J. Mol. Graphics Modelling*, **2001**, 19(1), 13–25.
- [8] Torrie, G.; Valleau, J. *J. Comput. Phys.*, **1977**, 23(2), 187–199.
- [9] Ferrenberg, A.; Swendsen, R. *Phys. Rev. Lett.*, **1989**, 63, 1195–1021.
- [10] Roux, B. *Comput. Phys. Commun.*, **1995**, 91, 275–282.
- [11] Hummer, G.; Szabo, A. *Proc. Natl. Acad. Sci. U.S.A.*, **2001**, 98(7), 3658–3661.
- [12] Hummer, G.; Szabo, A. *Acc. Chem. Res.*, **2005**, 38(7), 504–513.
- [13] Park, S.; Khalili-araghi, F.; Tajkhorshid, E.; Schulten, K. *J. Chem. Phys.*, **2003**, 119(6), 3559–3566.
- [14] Park, S.; Schulten, K. *J. Chem. Phys.*, **2004**, 120(13), 5946–5961.
- [15] Cover, T.; Thomas, J. *Elements of Information Theory*. Wiley, John, & Sons, Inc., 2 edition, 2006.
- [16] Jarzynski, C. *Phys. Rev. Lett.*, **1997**, 78(14), 2690–2693.
- [17] Jarzynski, C. *Phys. Rev. E*, **1997**, 56(5), 5018–5035.
- [18] Ermak, D.; McCammon, J. *J. Chem. Phys.*, **1978**, 69(4), 1352–1360.
- [19] Braun, O.; Hanke, A.; Seifert, U. *Phys. Rev. Lett.*, **2004**, 93(15), 158105.